Novel Cofacial Ruthenium(II) Porphyrin Dimers and Tetramers

Kenji Funatsu,[†] Taira Imamura,*[,†] Akio Ichimura,[‡] and Yoichi Sasaki[†]

Division of Chemistry, Graduate School of Science, Hokkaido University, Sapporo 060-0810, Japan, and Department of Chemistry, Faculty of Science, Osaka City University, Osaka 558-0022, Japan

Received October 28, 1997

A series of cofacially arranged ruthenium(II) porphyrin dimers **1**−**5** having a variety of axial ligands such as CO, pyridine, and 4-cyanopyridine, were synthesized. Porphyrin tetramers, **6** and **7**, which have pyridylporphyrin ligands at the axial positions of the parent cofacial ruthenium(II) dimers, were also prepared. These porphyrin dimers and tetramers were characterized by ^{1}H NMR spectroscopy, ESI (electrospray ionization)−mass spectroscopy, and elemental analysis. The ruthenium porphyrin dimers and tetramers exhibited characteristic electrochemical and spectroscopic properties caused by interactions between the porphyrin subunits. Stepwise oxidations of the porphyrin rings or the ruthenium ions in the cofacial dimer skeltons were observed in the cyclic voltammograms. The potential differences ($\Delta E^{\circ\prime}$ mV) of the oxidation steps were larger than 260 mV for all the porphyrin oligomers. The Soret bands of the cofacial dimers were significantly broadened by excitonic interactions between the two porphyrin subunits. Furthermore, the mixed-valence states of **3**−**7** showed specific intervalence charge-transfer (IT) bands between the Ru(II) and Ru(III) cores in the near-IR region at around 1500 nm.

Introduction

Assembly of multicomponents is essential for the construction of the functional systems such as molecular electronic devices, redox-active materials, and light-harvesting structures.[1] In addition, since the structure of the photosynthetic reaction center of *Rhodopseudomonas vividis* was determined by X-ray crystallography,[2] many researchers have taken a great interest in experimental and theoretical examinations of the electronic structure of the photosynthetic reaction center.[3] Special attention has been paid to the two Bchlb molecules called "special pairs" which are arranged cofacially with an average ring separation ∼3.3 Å between the pyrrole rings I.[4] To mimic the "special pairs", many porphyrin dimers and oligomers bound covalently by organic spacers, such as phenyl substituents, were synthesized and their potential photochemical properties were sought.[4,5] Recently self-assembly of metal-porphyrins with pyridyl,[6,7] imidazolyl,[8] or oxo-substituents[9,10] were used for the construction of metal-porphyrin oligomers containing cofacially arranged zinc[6] and iron[9] porphyrin dimers. Crystal structures of the two zinc dimers $[Zn(2\text{-PyPOR})]_2$ showed that the pyrrole rings overlap each other, and the mean plane separations between the 24 atom porphyrin cores were ca. 3.3 Å.[6a] Hence the zinc

[†] Hokkaido University.
[‡] Osaka City University.

(1) For example: Balzani, V.; Scandola, F. In *Comprehensive Supramolecular Chemistry*; Atwood, J., MacNicol, D., Davies, E., Vögtle, F., Lehn J.-M., Eds.; Pergamon Press: Oxford, U.K., 1996; Vol. 10, p 687.

(2) (a) Deisenhofer, J.; Michel, H. *Science* **1989**, *245*, 1463. (b) Deisenhofer, J.; Epp, O.; Miki, K.; Huber, R.; Michel, H. *Nature* **1985**, *318*, 618.

(3) (a) Warshel, A.; Parson, W. W. *J. Am. Chem. Soc.* **1987**, *109*, 6243. (b) Warshel, A.; Parson, W. W. *J. Am. Chem. Soc.* **1987**, *109*, 6252. (c) Thompson, M. K.; Zerner, M. C.; Fajer, J. *J. Phys. Chem.* **1991**, *95*, 5693. (d) Lathrop, E. J. P.; Friesner, R. A. *J. Phys. Chem.* **1994**, *98*, 3056.

(4) (a) Sessler, J. L.; Johnson, M. R.; Lin, T. Y.; Creager, S. E. *J. Am. Chem. Soc.* **1988**, *110*, 3659. (b) Harriman, A.; Odobel, F., Sauvage, J. P. *J. Am. Chem. Soc.* **1994**, *116*, 5481. (c) Wasielewski, M. R.; Johnson, D. G.; Niemczyk, M. P.; Gaines, G. L., III; O'Neil, M. P.; Svec, W. A. *J. Am. Chem. Soc.* **1990**, *112*, 6482. (d) Osuka, A.; Nakajima, S.; Maruyama, K. *J. Org. Chem.* **1992**, *57*, 7255. (e) Markl, G.; Reiss, M.; Keitmeier, P.; Noth, H. *Angew. Chem., Int. Ed. Engl.* **1995**, *34*, 2230. (f) Chang, C. K.; Abdalmuhdi, I. *J. Org. Chem.* **1983**, *48*, 5388. (g) Tabushi, I.; Sasaki, T. *Tetrahedron Lett.* **1982**, 23, 1913. (h) Sessler, J. L.; Johnson, M. R.; Creager, S. E.; Fettinger, J. C.; Ibers, J. A. *J. Am. Chem. Soc.* **1990**, *112*, 9310. (i) Senge, O. M.; Gerzevske, K. R.; Vicente, M. G. H.; Forsyth, T. P.; Smith, K. M. *Angew. Chem., Int. Ed. Engl.* **1993**, *32*, 750. (j) Burrell, A. K.; Officer, D. L.; Reid, D. C. W. *Angew. Chem., Int. Ed. Engl.* **1995**, *34*, 900. (k) Chambron, J. C.; Heutz. V.; Sauvage, J. P. *Bull. Soc. Chim. Fr.* **1995**, *132*, 340. (l) Kurreck, H.; Huber, M. *Angew. Chem., Int. Ed. Engl.* **1995**, *34*, 849. (m) Autret, M.; Plouzennec, L. M.; Moinet, C.; Simonneaux, G. *J. Chem. Soc., Chem. Commun.* **1994**, 1169. (n) Tamiaki, H. *Coord. Chem. Rev.* **1996**, *148*, 183.

(5) (a) Osuka, A.; Maruyama, K. *J. Am. Chem. Soc.* **1988**, *110*, 4454. (b) Won, Y.; Friesner, R. A.; Johnson, M. R.; Sessler, J. L. *Photosynth. Res.* **1989**, 201. (c) Hunter, C. A.; Sanders, J. K. M.; Stone, A. J. *Chem. Phys.* **1989**, *133*, 395. (d) Tran-Thi, T. H.; Lipskier, J. F.; Maillard, P.; Momenteau, M.; Lopez-Gastillo, J.-M.; Jay-Grein, J.-P. *J. Phys. Chem.* **1992**, *96*, 1073.

(6) (a) Stibrany, R. T.; Vasudevan, J.; Knapp, S.; Potenza, J. A.; Emge, T.; Schugar, H. J. *J. Am. Chem. Soc.* **1996**, *118*, 3980. (b) Chi, X.; Guerin, A. J.; Haycock, R. A.; Hunter, C. A.; Sarson, L. D. *J. Chem. Soc., Chem. Commun.* **1995**, 2563. (c) Chi, X.; Guerin, A. J.; Haycock, R. A.; Hunter, C. A.; Sarson, L. D. *J. Chem. Soc., Chem. Commun.* **1995**, 2567.

(7) (a) Drain, C. M.; Lehn, L.-M. *J. Chem. Soc., Chem. Commun.* **1994**, 2313. (b) Fleischer, E. B.; Shachter, A. M. *Inorg. Chem.* **1991**, *30*, 3763. (c) Funatsu, K.; Kimura, A.; Imamura, T.; Sasaki, Y. *Chem. Lett.* **1995**, 765. (d) Hunter, C. A.; Hyde, R. K. *Angew. Chem., Int. Ed. Engl.* **1996**, *35*, 1936.

(8) (a) Kokube, Y.; Miyaji, H. *J. Am. Chem. Soc.* **1994**, *116*, 4111. (b) Kokube, Y.; Miyaji, H. *Bull. Chem. Soc. Jpn.* **1996**, 69, 3563.

(9) (a) Goff, H. M.; Shimomura, E. T.; Lee, Y. J.; Scheidt, W. R. *Inorg. Chem.* **1984**, *23*, 315. (b) Godziela, G. M.; Tilotta, D.; Goff, H. M. *Inorg. Chem.* **1986**, *25*, 2142. (c) Balch, A. L.; Latos-Grażyński, L.; Noll, B. C.; Olmstead, M. M.; Zovinka, E. P. *Inorg. Chem.* **1992**, *31*, 2148. (d) Balch, A. L.; Latos-Grażyński, L.; St. Claire, T. N. *Inorg. Chem.* **1995**, *34*, 1395. (e) Balaban, T. S.; Tamiaki, H.; Holzwarth, A. R.; Schaffner, K. *J. Phys. Chem. B* **1997**, *101*, 3424.

(10) (a) Wojaczynski, J.; Latos-Grażyński, L. *Inorg. Chem.* **1996**, *35*, 4812. (b) Wojaczynski, J.; Latos-Grażyński, L. *Inorg. Chem.* **1995**, *34*, 1054. (c) Wojaczynski, J.; Latos-Grażyński, L. *Inorg. Chem.* **1995**, *34*, 1044.

S0020-1669(97)01361-X CCC: $15.00
Published on Web 08/29/1998

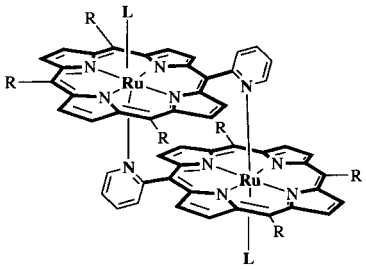

1 (L = CO, R = tolyl)
2 (L = CO, R = 4-tert-butylphenyl)
3 (L = Py, R = tolyl)
4 (L = Py, R = 4-tert-butylphenyl)
5 (L = PyCN, R = 4-tert-butylphenyl)

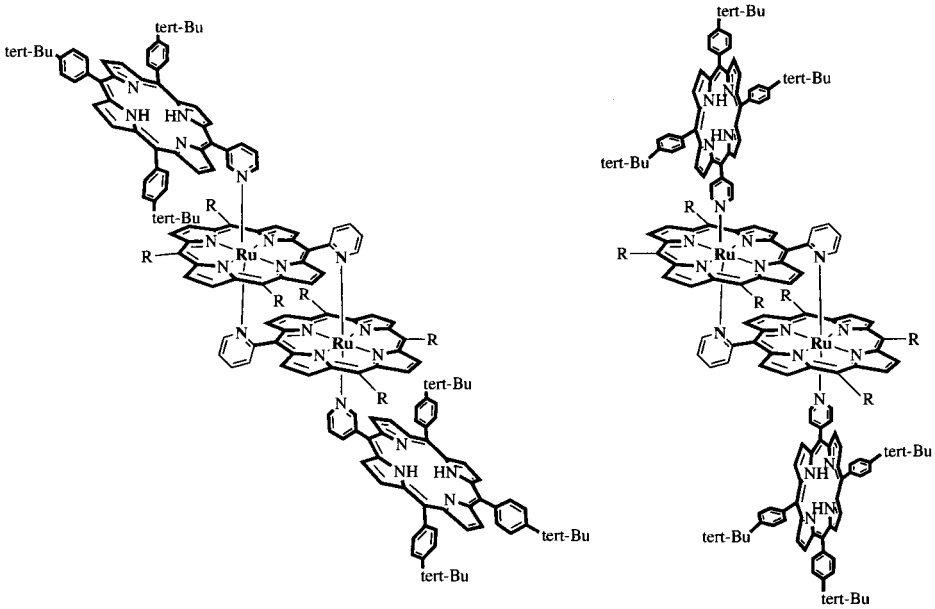

6 (R = tolyl) **7** (R = tolyl)

Figure 1. Structures of cofacially arranged ruthenium(II) porphyrin dimers and tetramers.

dimers capture the structural character of "special pairs". Unfortunately, zinc(II) ion is relatively labile for substitution, and the zinc−porphyrin oligomers in solution are in equilibrium with monomers. Therefore we have paid more attention to the less labile metal ions of ruthenium(II) and osmium(II). A variety of perpendicularly linked ruthenium(II) and osmium(II) porphyrin oligomers were synthesized and investigated.[7c,11] We report herein the synthesis, characterization, and singular spectral and electrochemical properties of a new series of cofacially arranged ruthenium porphyrin dimers with axial ligands of CO, pyridine, or 4-cyanopyridine (isonicotinonitrile, PyCN), **1**−**5** as shown in Figure 1. Porphyrin tetramers, **6** and **7**, derived from the cofacial porphyrin dimers, are also reported.

Experimental Section

Materials. Pyrrole and *p*-tolualdehyde for the preparation of porphyrins, H_2(2-Py)T_3P, H_2(2-Py)tB_3P, H_2(3-Py)tB_3P, and H_2(4-Py)-tB_3P,[12] were purchased from Wako and used without further purification. 4-*tert*-Butylbenzaldehyde and 2-, 3-, and 4-pyridinecarbaldehyde for the preparation of the porphyrins were purchased from Aldrich. Triruthenium(0) dodecacarbonyl, $Ru_3(CO)_{12}$, and H_2OEP were also purchased from Aldrich. Ethanol was purified by distillation under N_2 gas after dehydration using 4-Å molecular sieves. Dichloromethane and toluene were used without further purification. Silica gel (Wakogel C-300) and alumina (Wolem, neutral, activity III) were used for column chromatography. TLC silica plates were purchased from Tokyo Kasei.

Measurements. ^{1}H NMR spectra were recorded on a JEOL-EX270 spectrometer. IR spectra (KBr method) were measured with a Hitachi 270−50 infrared spectrophotometer. UV−vis spectra were recorded on a Hitachi U-3410 or U-3000 spectrophotometer. Near-IR absorption spectra were also recorded on a Hitachi U-3410 spectrophotometer. Cyclic voltammetry (CV) and differential pulse voltammetry (DPV) were performed with a BAS CV-50W voltammetry analyzer. The data were digitized and stored in a personal computer. The working and the counter electrodes for the cyclic voltammetry measurements were a platinum disk (i.d. = 1.6 mm) and a platinum wire, respectively. Cyclic voltammograms and differential pulse voltammograms were recorded at a scan rate of 100 and 30 mV/s at 20 °C, respectively. The

(11) (a) Kimura, A.; Funatsu, K.; Imamura, T.; Kido, H.; Sasaki, Y. *Chem. Lett.* **1995**, 207. (b) Funatsu, K.; Kimura, A.; Imamura, T.; Ichimura, A.; Sasaki, Y. *Inorg. Chem.* **1997**, *36*, 1625. (c) Kariya, N.; Imamura, T.; Sasaki, Y. *Inorg. Chem.* **1997**, *36*, 833.

(12) Abbreviations: OEP = 2,3,7,8,12,13,17,18-octaethylporphyrinato dianion; TPP = 5,10,15,20-tetraphenylporphyrinato dianion; TTP=5,-10,15,20-tetratolylporphyrinato dianion; 4-PyT_3P = 5-(4-pyridyl)-10,15,20-tritolylporphyrinato dianion; POR = general porphyrin dianion; H_2tB_4P = 5,10,15,20-tetra(4-*tert*-butyl)phenylporphyrin; H_2-(4-Py)P_3P = 5-(4-pyridyl)-10,15,20-triphenylporphyrin; H_2(2-Py)T_3P = 5-(2-pyridyl)-10,15,20-tritolylporphyrin; H_2(2-Py)tB_3P = 5-(2-pyridyl)-10,15,20-tri(4-*tert*-butyl)phenylporphyrin; H_2(3-Py)tB_3P = 5-(3-pyridyl)-10,15,20-tri(4-*tert*-butyl)phenylporphyrin; H_2(4-Py)tB_3P = 5-(4-pyridyl)-10,15,20-tri(4-*tert*-butyl)phenylporphyrin; Py = pyridine; PyCN = 4-cyanopyridine (isonicotinonitrile); azpy = 4,4′-azopyridine; TBA(PF_6) = *n*-tetrabutylammonium hexafluorophosphate; CV = cyclic voltammogram; DPV = differential pulse voltammogram.

sample solutions in 0.1 M (TBA)PF_6·CH_2Cl_2 ((TBA)PF_6 = tetrabutylammonium hexafluorophosphate) were deoxygenated by a stream of argon. The reference electrode was Ag/0.01 M [$Ag(CH_3CN)_2$]PF_6, 0.1 M (TBA)PF_6 (acetonitrile), or Ag/AgCl. Redox potentials obtained were corrected by the potential of a ferrocenium/ferrocene couple (0.352 V).

Synthesis of Porphyrins, H_2(2-Py)T_3P, H_2(2-Py)tB_3P, H_2(3-Py)tB_3P, and H_2(4-Py)tB_3P. Porphyrins containing *meso*-pyridyl groups were synthesized with reference to the literature method of *meso*-pyridyl derivatives of tetraphenylporphyrin.[7b,c,11]

H_2(2-Py)T_3P. *p*-Tolualdehyde (15 mL), 2-pyridinecarbaldehyde (4.2 mL), and pyrrole (10.3 mL) were condensed in 200 mL of refluxing propionic acid. The crystalline product of a porphyrin mixture (2.95 g) was obtained after cooling the solution. The monopyridylporphyrin of H_2(2-Py)T_3P was isolated by silica gel chromatography. The amount of H_2(2-Py)T_3P was 0.83 g (yield: 28%). The desired porphyrin was identified by thin-layer chromatography, elemental analysis, and ^{1}H NMR measurements. Anal. Calcd for $C_{46}H_{35}N_5$: C, 83.99; H, 5.36; N, 10.65. Found: C, 84.07; H, 5.28; N, 10.69. ^{1}H NMR ($CDCl_3$, 270 MHz): H_{NH} δ −2.77 (s, 2H), H_{CH3} 2.65 (s, 9H), H_β 8.88 (m, 8H), H_o 8.09 (d, J = 7.9 Hz, 6H), H_m 7.55 (d, J = 7.9 Hz, 6H), H_{Py} 9.13 (m, 1H), 8.24 (m, 1H), 8.07 (m, 1H), 7.70 (m, 1H) ppm.

H_2(2-Py)tB_3P was synthesized by replacing *p*-tolualdehyde with 4-*tert*-butylbenzaldehyde used in the synthesis of H_2(2-Py)T_3P. 4-*Tert*-butylbenzaldehyde (12.5 mL), 2-pyridinecarbaldehyde (2.3 mL), and pyrrole (6.7 mL) were used. A porphyrin mixture (2.20 g) was obtained. The mixture was separated by using a silica gel column. At first H_2tB_4P was eluted by CH_2Cl_2, and was used for the preparation of the ruthenium porphyrin monomers of Ru(tB_4P)(CO)(MeOH), Ru(tB_4P)(CO)(Py), Ru(tB_4P)$(Py)_2$, and Ru(tB_4P)$(PyCN)_2$. The amount of H_2tB_4P was 1.0 g. Then H_2(2-Py)tB_3P was eluted by CH_2Cl_2 containing 2% EtOH. The amount of H_2(2-Py)tB_3P was 0.45 g (yield: 20%). Anal. Calcd for $C_{55}H_{53}N_5$: C, 84.25; H, 6.81; N, 8.93. Found: C, 84.15, H, 6.87, N, 8.66. ^{1}H NMR ($CDCl_3$, 270 MHz): H_{NH} δ −2.75 (s, 2H), $H_{tert-Bu}$ 1.61 (s, 27H), H_β 8.88 (m, 8H), H_o 8.15 (d, J = 8.2 Hz, 6H), H_m 7.76 (d, J = 8.2 Hz, 6H), H_{Py} 9.14 (m, 1H), 8.26 (m, 1H), 8.10 (m, 1H), 7.72 (m, 1H).

H_2(3-Py)tB_3P. 4-*tert*-Butylbenzaldehyde (12.5 mL), 3-pyridinecarbaldehyde (2.3 mL), and pyrrole (6.7 mL) were used. A purple product of a porphyrin mixture (1.55 g) was obtained. The amount of purified H_2(3-Py)tB_3P was 0.3 g (yield: 20%). Anal. Calcd for $C_{55}H_{53}N_5$: C, 84.25; H, 6.81; N, 8.93. Found: C, 83.81, H, 7.01, N, 8.52. ^{1}H NMR ($CDCl_3$, 270 MHz): H_{NH} δ −2.76 (s, 2H), $H_{tert-Bu}$ 1.61 (s, 27H), H_β 8.89 (m, 8H), H_o 8.15 (d, J = 7.9 Hz, 6H), H_m 7.77 (d, J = 7.9 Hz, 6H), H_{Py} 9.47 (m, 1H), 9.04 (m, 1H), 8.53 (m, 1H), 7.75 (m, 1H).

H_2(4-Py)tB_3P. 4-*tert*-Butylbenzaldehyde (5.0 mL), 4-pyridinecarbaldehyde (0.95 mL), and pyrrole (2.76 mL) were used. The purified H_2(4-Py)tB_3P (yield: 0.15 g, 16%) was obtained from a purple porphyrin mixture (0.96 g). Anal. Calcd for $C_{55}H_{53}N_5$: C, 84.25; H, 6.81; N, 8.93. Found: C, 83.96, H, 6.70, N, 8.89. ^{1}H NMR ($CDCl_3$, 270 MHz): H_{NH} δ −2.78 (s, 2H), $H_{tert-Bu}$ 1.61 (s, 27H), H_β 8.88 (m, 8H), H_o 8.14 (d, J = 8.3 Hz, 6H), H_m 7.76 (d, J = 8.3 Hz, 6H), H_{Py} 9.03 (dd, 2H), 8.17 (dd, 2H).

Synthesis of Monomers. Ruthenium porphyrin monomers were synthesized with reference to the literature methods of Ru(TPP)(CO)(EtOH),[13a] Ru(OEP)(CO)(MeOH),[13a] Ru(OEP)(CO)(Py),[14] and Ru(OEP)$(Py)_2$.[14]

Ru(tB_4P)(CO)(MeOH). Anal. Calcd for $C_{62}H_{64}N_4O_2Ru$: C, 74.59; H, 6.46; N, 5.61. Found: C, 74.88; H, 6.80; N, 5.79. UV−vis (CH_2Cl_2): λ_{max}/nm 413 (Soret), 532. IR (KBr): ν_{CO} 1946 cm^{-1}. ^{1}H NMR ($CDCl_3$−2% CD_3OD, 270 MHz): H_β δ 8.71 (s); H_o 8.04, 8.14 (d, 7.92 Hz); H_m 7.72 (d, 7.92 Hz); $H_{tert-Bu}$ 1.60 (s).

Ru(OEP)(CO)(MeOH). Anal. Calcd for $C_{38}H_{48}N_4O_2Ru$: C, 65.77; H, 6.97; N, 8.08. Found: C, 66.00; H, 7.01; N, 7.93. UV−vis (CH_2Cl_2): λ_{max}/nm 392 (Soret), 517, 548. IR (KBr): ν_{CO} 1950, 1923 cm^{-1}. ^{1}H NMR (CD_2Cl_2−2% CD_3OD, 270 MHz): H_{meso} δ 9.95 (s); CH_3CH_2 4.11 (q, 7.56 Hz); CH_3CH_2 1.94 (t, 7.56 Hz).

Ru(tB_4P)(CO)(Py). Anal. Calcd for $C_{66}H_{65}N_5ORu$: C, 75.83; H, 6.27; N, 6.70. Found: C, 75.99; H, 6.18; N, 6.89. UV−vis (CH_2Cl_2): λ_{max}/nm 414 (Soret), 534, 568. IR (KBr): ν_{CO} 1948 cm^{-1}. ^{1}H NMR ($CDCl_3$, 270 MHz): H_{Py} δ 1.49 (d), 5.15 (t), 6.05 (t); H_β 8.64 (s); H_o 7.95, 8.15 (d, 7.92 Hz); H_m 7.66, 7.72 (d, 7.92 Hz); $H_{tert-Bu}$ 1.59 (s).

Ru(tB_4P)$(Py)_2$. Anal. Calcd for $C_{70}H_{70}N_6Ru$: C, 76.68; H, 6.44; N, 7.67. Found: C, 76.41; H, 6.77; N, 7.89. UV−vis (CH_2Cl_2): λ_{max}/nm 413, 422 (Soret), 506. ^{1}H NMR (C_6D_6, 270 MHz): H_{Py} δ 2.94 (d), 4.51 (t), 5.08 (t); H_β 8.69 (s); H_o 8.28 (d, 8.25 Hz); H_m 7.61 (d, 8.25 Hz); $H_{tert-Bu}$ 1.44 (s).

Ru(tB_4P)$(PyCN)_2$. Anal. Calcd for $C_{72}H_{68}N_8Ru$: C, 75.43; H, 5.98; N, 9.78. Found: C, 75.61; H, 6.18; N, 9.89. UV−vis (CH_2Cl_2): λ_{max}/nm 407, 418 (Soret), 509, 550−650. IR (KBr): ν_{CN} 2236 cm^{-1}. ^{1}H NMR (C_6D_6, 270 MHz): H_{Py} δ 2.30 (d), 3.86 (d); H_β 8.80 (s); H_o 8.83 (d, 8.25 Hz); H_m 7.72 (d, 8.25 Hz); $H_{tert-Bu}$ 1.47 (s).

Ru(OEP)$(PyCN)_2$. Anal. Calcd for $C_{48}H_{52}N_6Ru$: C, 70.82; H, 6.44; N, 10.33. Found: C, 71.13; H, 6.71; N, 10.50. UV−vis (CH_2Cl_2): λ_{max}/nm 399 (Soret), 498, 525, 618. IR (KBr): ν_{CN} 2230 cm^{-1}. ^{1}H NMR ($CDCl_3$, 270 MHz): H_{py} δ 1.46 (d), 4.93 (d); H_{meso} 9.40 (s); CH_3CH_2 3.85 (q, 7.59 Hz); CH_3CH_2 1.80 (t, 7.59 Hz).

Synthesis of Cofacial Dimers and Tetramers. [Ru(2-PyT_3P)(CO)]$_2$ (1). Diethylene glycol monomethyl ether suspension (100 mL) containing H_2(2-Py)T_3P (35 mg, 5.32×10^{-5} mol) and $Ru_3(CO)_{12}$ (100 mg, 1.56×10^{-4} mol) was refluxed for 2 h under N_2 atmosphere. The reaction was stopped when the characteristic visible spectral band of H_2(2-Py)T_3P around 650 nm was no longer evident. The solution was cooled and filtered. To the solution, 100 mL of a saturated NaCl aqueous solution was added. The resulting precipitate was filtered through a sintered glass funnel, washed with water, and dried at 100 °C in vacuo for 1 h. Because the crude product in solution exhibited an extra band around 610 nm, because of a chlorin impurity, DDQ (2,3-dichloro-5,6-dicyano-1,4-benzoquinone) was added to the dichloromethane solution of the crude product, and the suspension was stirred at room temperature until the band was disappeared.[13] The suspension was filtered to remove insoluble materials, and the filtrate was chromatographed on a silica gel column with toluene as an eluent. The first eluted band was collected and evaporated to dryness. The product was dried at 80 °C in vacuo for 3 h (yield: 9 mg, 22%) Anal. Calcd for $C_{94}H_{66}N_{10}O_2Ru_2$: C, 71.92; H, 4.24; N, 8.92. Found: C, 71.79; H, 4.36; N, 8.76. ^{1}H NMR ($CDCl_3$, 270 MHz): H_{Py} δ 1.82 (m, 2H), 5.75 (m, 4H), 6.33 (m, 2H), H_β 5.36 (d, 4.95 Hz, 4H), 8.15 (d, 4.95 Hz, 4H), 8.76 (d, 4.95 Hz, 4H), 8.82 (d, 4.95 Hz, 4H), H_o 7.91, 8.06, 8.44−8.51 (m, 12H), H_m 7.51−7.60, 7.65−7.74 (m, 12H), H_{tolyl} 2.78 (s, 6H), 2.80 (s, 12H).

[Ru(2-PytB_3P)(CO)]$_2$ (2). [Ru(2-PytB_3P)(CO)]$_2$ was synthesized by a method similar to that of [Ru(2-PyT_3P)(CO)]$_2$ using H_2(2-Py)tB_3P in place of H_2(2-Py)T_3P. $Ru_3(CO)_{12}$ (100 mg, 1.56×10^{-4} mol) and H_2(2-Py)tB_3P (60 mg, 7.61×10^{-5} mol) were used (yield: 20 mg, 29%). Anal. Calcd for $C_{112}H_{102}N_{10}O_2Ru_2$: C, 73.82; H, 5.64; N, 7.69. Found: C, 73.79; H, 5.84; N, 7.79. ^{1}H NMR ($CDCl_3$, 270 MHz): H_{Py} δ 1.79 (m, 2H), 5.74 (m, 4H), 6.33 (m, 2H), H_β 5.38 (d, J = 4.95 Hz, 4H), 8.18 (d, J = 4.95 Hz, 4H), 8.79 (d, J = 4.95 Hz, 4H), 8.85 (d, J = 4.95 Hz, 4H), $H_{o,m}$ 8.56 (m, 4H), 7.71−8.14 (m, 20H), $H_{tert-Bu}$ 1.68 (s, 18H), 1.69 (s, 36H).

[Ru(2-PyT_3P)(Py)]$_2$ (3). In the synthesis of [Ru(2-PyPOR)(L)]$_2$ (L = Py, PyCN, $H_2$3-PytB_3P, $H_2$4-PytB_3P), the toluene solution containing the parent complex of [Ru(2-PyPOR)(CO)]$_2$ and a corresponding ligand L was photoirradiated using a medium-pressure mercury lamp. In **3**, the solution (700 mL) containing [Ru(2-PyT_3P)(CO)]$_2$ (32 mg, 2.04×10^{-5} mol) and pyridine (3.5 μL, 4.08×10^{-5} mol) was irradiated for 2 h with stirring and vigorous Ar bubbling[14] at the temperatures between 0 and 5 °C. The solution was changed in color from red to brown upon irradiation. The brown solution was filtered and evaporated to dryness. The resulting solid was dissolved in a small amount of toluene and separated by an alumina column (activity III) with toluene as an eluent. The first eluted brown band was collected and evaporated to dryness. The resulting deep-purple solid was recystallized from toluene-methanol, and dried at 110 °C in vacuo for 2 h (yield: 28 mg, 82%).

(13) (a) Collman, J. P.; Barnes, C. E.; Brothers, P. J.; Collins, T. J.; Ozawa, T.; Gallucci, J. C.; Ibers, J. A. *J. Am. Chem. Soc.* **1984**, *106*, 5151. (b) Rousseau, K.; Dolphin, D. *Tetrahedron Lett.* **1974**, 4251.

(14) (a) Antipas, A.; Buchler, J. W.; Gouterman, M.; Smith, P. D. *J. Am. Chem. Soc.* **1978**, *100*, 3015. (b) Sovocol, W.; Hopf, E. R.; Whitten, D. G. *J. Am. Chem. Soc.* **1972**, *94*, 4350.

Anal. Calcd for $C_{102}H_{76}N_{12}Ru_2$: C, 73.23; H, 4.64; N, 10.05. Found: C, 73.40; H, 4.83; N, 9.83.

[Ru(2-PytB$_3$P)(Py)]$_2$ (4). [Ru(2-PytB$_3$P)(Py)]$_2$ was synthesized using [Ru(2-PytB$_3$P)(CO)]$_2$ in place of [Ru(2-PyT$_3$P)(CO)]$_2$. [Ru(2-PytB$_3$P)(CO)]$_2$ (25 mg, 1.37×10^{-5} mol) and pyridine (2.2 μL, 2.75×10^{-5} mol) were used (yield: 23.5 mg, 89%). Anal. Calcd for $C_{120}H_{112}N_{12}Ru_2$: C, 74.89; H, 5.87; N, 8.74. Found: C, 74.81; H, 6.35; N, 8.23. ^{1}H NMR (C_6D_6, 270 MHz): H_{Py} δ 3.47 (d, 2H), 5.14 (t, 2H), 5.46 (m, 4H), $H_{\alpha-Py}$ 1.86 (d, 4H), $H_{\beta-Py}$ 4.05 (t, 4H), $H_{\gamma-Py}$ 4.72 (t, 2H), H_β 5.97 (d, J = 4.95 Hz, 4H), 8.50 (d, J = 4.95 Hz, 4H), 8.93 (m, 8H), $H_{o,m}$ 8.93−8.81 (dd, J = 1.65, 7.92 Hz, 4H), 8.34−7.62 (dd, J = 1.65, 7.92 Hz, 20H), $H_{tert-Bu}$ 1.62 (s, 36H), 1.54 (s, 18H).

[Ru(2-PytB$_3$P)(PyCN)]$_2$ (5). [Ru(2-PytB$_3$P)(CO)]$_2$ (26 mg, 1.43×10^{-5} mol) and 4-cyanopyridine (3.0 mg, 2.88×10^{-5}mol) were used (yield: 23.0 mg, 81%). Anal. Calcd for $C_{122}H_{110}N_{14}Ru_2$: C, 74.21; H, 5.62; N, 9.93. Found: C, 74.16; H, 5.88; N, 9.67. ^{1}H NMR (C_6D_5-CD_3, 270 MHz): H_{Py} δ 3.11 (d, 2H), 5.16 (t, 2H), 5.54 (d, 4H), 5.62 (t, 2H), $H_{\alpha-Py}$ 1.32 (dd, 4H), $H_{\beta-Py}$ 3.63 (dd, 4H), H_β 5.76 (d, J = 4.95 Hz, 4H), 8.36 (d, J = 4.95 Hz, 4H), 8.79 (m, 8H), $H_{o,m}$ 7.76−8.76 (dd, J = 1.65, 7.92 Hz, 24H), $H_{tert-Bu}$ 1.65 (s, 36H), 1.58 (s, 18H). IR (KBr): ν_{CN} 2232 cm^{-1}.

[Ru(2-PyT$_3$P)(H$_2$3-PytB$_3$P)]$_2$ (6). The solution containing [Ru(2-PyT$_3$P)(CO)]$_2$ (27 mg, 1.72×10^{-5} mol) and H$_2$(3-Py)tB$_3$P (27 mg, 3.44×10^{-5} mol) was irradiated with UV−visible light for 3 h. The solution obtained was filtered. The resulting solid was dried, dissolved in a small amount of toluene, and purified by silica gel column chromatography using toluene as eluent. The first eluted brownish-purple band was collected and evaporated to dryness. The resulting deep-purple solid was dried at 100 °C in vacuo for 2 h (yield: 27 mg, 54%). Anal. Calcd for $C_{202}H_{172}N_{20}Ru_2$: C, 78.72; H, 5.63; N, 9.09. Found: C, 78.82; H, 6.00; N, 8.66. ^{1}H NMR (C_6D_6, 270 MHz): H_{Py} δ 3.22 (d, 2H), 3.64 (t, 2H), 4.40 (m, 2H), 4.50 (t, 2H), 2.30 (d, 2H), 6.02 (d, 2H), H_β 5.73 (d, J = 4.95 Hz, 4H), 8.25 (d, J = 4.95 Hz, 4H), 8.78 (d, 4H), 8.86 (d, 4H), 6.74 (d, 4H), 8.57 (d, 4H), 8.93 (d, 4H), 8.99 (d, 4H), $H_{o,m}$ 6.65−8.63 (dd, J = 1.65, 7.92 Hz, 48H), $H_{tert-Bu}$ 1.45 (s), 1.47 (s), H_{tolyl} 2.35 (s), 2.45 (s).

[Ru(2-PyT$_3$P)(H$_2$4-PytB$_3$P)]$_2$ (7). [Ru(2-PyT$_3$P)(CO)]$_2$ (27 mg, 1.72×10^{-5} mol) and H$_2$(4-Py)tB$_3$P (27 mg, 3.44×10^{-5} mol) were used (yield: 23 mg, 46%). Anal. Calcd for $C_{202}H_{172}N_{20}Ru_2$: C, 78.72; H, 5.63; N, 9.09. Found: C, 78.56; H, 6.02; N, 8.84. ^{1}H NMR (C_6D_6, 270 MHz): H_{Py} δ 3.70 (d, 2H), 5.23 (t, 2H), 5.67 (t, 2H), 5.94 (d, 2H), 2.29 (d, 4H), 5.08 (d, 4H), H_β 6.99 (d, J = 4.95 Hz, 4H), 8.43 (d, J = 4.95 Hz, 4H), 8.85 (m, 8H), 6.21 (d, 4H), 8.54 (d, 4H), 9.07 (m, 8H), $H_{o,m}$ 7.04−8.85 (dd, J = 1.65, 7.92 Hz, 48H), $H_{tert-Bu}$ 1.41 (s), 1.45 (s), H_{tolyl} 2.55 (s), 2.58 (s).

Results and Discussion

Characterization of Ruthenium Porphyrin Oligomers, 1−7. With the exception of the cofacial bispyridine dimer **3**, the other cofacial ruthenium porphyrin dimers were characterized by ^{1}H NMR spectroscopy, IR spectroscopy, electrospray ionization mass spectrometry (ESI-MS), and microanalysis. In the case of **3**, much lower solubility than the other cofacial dimers made accurate analyses of the ^{1}H NMR spectra difficult. However, all the data from ESI-MS and microanalysis, and the similarities in the UV−vis spectral and cyclic voltammetric features of **3** and **4** supported the formation of a cofacial dimeric structure for **3**.

Cofacial Carbonyl Dimers, 1 and 2. Solubility of both the cofacial carbonyl dimers in nonpolar solvents such as dichloromethane, chloroform, toluene, and benzene was unexpectedly similar, though the solubility of the dimer **2** with *tert*-butyl substituents, was much lower than that of a monomeric analogue of Ru(TPP)(CO)(Py). Elemental analyses of the cofacial carbonyl dimers agreed well with their respective compositions as detailed in the Experimental Section. Infrared spectra of **1** and **2** showed characteristic carbonyl stretches around 1955 cm^{-1}. This value is almost the same as those of a monomer analogue Ru(TPP)(CO)(Py)[15] and perpendicularly linked ruthenium porphyrin oligomers.[11] ESI-MS exhibited fragment peaks at molecular weights of the cofacial carbonyl dimers, **1** and **2**, at m/z^+ 1570.8 (relative abundance: 92%) and 1824.0 (25%), respectively. ^{1}H NMR spectra were especially diagnostic for the structure of the cofacial ruthenium porphyrin dimers. The signal patterns of **1** and **2** are almost the same as each other, except the signals of the *meso*-phenyl substituents. In both systems, four 2-pyridyl protons and four β-pyrrole protons were observed in a significantly higher region due to the shielding effect of the facing porphyrin π-conjugated system, as observed in the similar zinc cofacial dimer systems.[6a] Although some signals of the 2-pyridyl protons overlapped, integral intensities of the signals and the signal correlation on H−H COSY measurements cleaned up the problem. The chemical shift values of **1** and **2** are listed in Table 1.

Cofacial Bispyridine Dimers, 3 and 4. Infrared spectra of **3** and **4** showed no carbonyl stretches, indicating the complete replacement of carbonyl ligands by pyridine in the synthetic procedures. Solubility of **4** in nonpolar solvents such as toluene was much higher than that of **3** due to the solubility effect of *tert*-butyl substituents, which was in contrast to the case of the cofacial carbonyl dimers, **1** and **2**. ESI-MS was a very useful tool for the characterization of these cofacial porphyrin dimers as has been often used to characterize multinuclear metal complexes.[16] ESI-MS exhibited fragment peaks corresponding to the molecular weights of both the dimers with 100% relative abundances, that is, m/z^+ = 1672.3 for **3** and 1923.3 for **4**. ^{1}H NMR spectra certified the cofacial structure of **4** depicted in Figure 1. The solubility in C_6D_6 was high enough for the measurements. The integral intensity ratios and the signal correlations obtained by H−H COSY measurements distinguished the 2-pyridyl and axial pyridine signals (Figure S1). Similarly to the carbonyl dimers of **1** and **2**, the 2-pyridyl and β-pyrrole proton signals of **4** were observed in the high magnetic field region at 1−6 ppm as listed in Table 1. Besides the four signals of 2-pyridyl protons, the three proton signals of α-(4H), β-(4H), and γ-positions (2H) of the axial pyridine ligands were also observed in the high magnetic region of 1 to 5 ppm, which are significantly higher than those of free pyridine signals (7−9 ppm).

Cofacial Bis(4-cyano)pyridine Dimer, 5. Cofacial bis(4-cyano)pyridine dimer, **5**, was fairly soluble in dichloromethane, chloroform, toluene, and benzene. Elemental analysis of **5** satisfied the composition. ESI-MS exhibited a fragment corresponding to the molecular weight of **5** (m/z^+ 1974.6) with 100% relative abundance. The ^{1}H NMR spectrum of **5** showed a β-pyrrole signal and four 2-pyridyl proton signals in the high magnetic field (1−6 ppm), as listed in Table 1, which was similar to the other cofacia dimers. Two double-doublet signals of the 4-cyanopyridine protons also appeared in the magnetic field (1.32 and 3.63 ppm) significantly higher than those of free 4-cyanopyridine (7.55 and 8.83 ppm in $CDCl_3$). The fact that only four 2-pyridyl and two 4-cyanopyridine proton signals were

(15) (a) Bonnet, J. J.; Eaton, S. S.; Eaton, G. R.; Holm, R. H.; Ibers, J. A. *J. Am. Chem. Soc.* **1973**, *95*, 2141. (b) Little, R. G.; Ibers, J. A. *J. Am. Chem. Soc.* **1973**, *95*, 8583.

(16) (a) Manna, J.; Whiteford, J. A.; Stang, P. J.; Muddiman, D. C.; Smith, R. D. *J. Am. Chem. Soc.* **1996**, *118*, 8731. (b) Stang, P. J.; Cao, D. H.; Chen, K.; Gray, G. M.; Muddiman, D. C.; Smith, R. D. *J. Am. Chem. Soc.* **1997**, *119*, 5163. (c) Fujita, M.; Nagao, S.; Ogura, K. *J. Am. Chem. Soc.* **1995**, *117*, 1649. (d) Whiteford, J. A.; Rachlin, E. M.; Stang, P. J. *Angew. Chem., Int. Ed. Engl.* **1996**, *35*, 2524. (e) Stang, P. J.; Persky, N. E. *J. Chem. Soc., Chem. Commun*. **1997**, 77. (f) Romero, M. F.; Ziessel, R.; D-Gervais, A.; Dorsseelaer, A. V. *J. Chem. Soc., Chem. Commun*. **1996**, 551.

Table 1. ^{1}H NMR Chemical Shift Values of Ruthenium(II) Porphyrin Dimers and Tetramers at 23 °C

complex (solvent)	2-pyridyl	β-pyrrole	phenyl (*o*, *m*)	tolyl(CH_3) or *tert*-Bu	pyridine or pyridyl (axial ligand)	NH
$[Ru(2\text{-}Py)T_3P)(CO)]_2$ (**1**)	1.82 (d, 2H)	5.36 (d. 4H)	7.51−8.51	2.78 (s)		
	5.75 (m, 4H)	8.15 (d, 4H)		2.80 (s)		
($CDCl_3$)	6.33 (t, 2H)	8.76 (d, 4H)				
		8.82 (d, 4H)				
δ/ppm vs TMS 0 ppm						
$[Ru(2\text{-}PytB_3P)(CO)]_2$ (**2**)	1.79 (d, 2H)	5.38 (d, 4H)	7.70−8.56	1.68 (s)		
	5.74 (m, 4H)	8.18 (d, 4H)		1.69 (s)		
($CDCl_3$)	6.33 (t, 2H)	8.79 (d, 4H)				
		8.85 (d, 4H)				
δ/ppm vs TMS 0 ppm						
$[Ru(2\text{-}PytB_3P)(Py)]_2$ (**4**)	3.47 (d, 2H)	5.97 (d, 4H)	7.62−8.93	1.54 (s)	1.86 (d, 4H)	
(C_6D_6)	5.14 (t, 2H)	8.50 (d, 4H)		1.62 (s)	4.05 (t, 4H)	
δ/ppm vs C_6H_6 7.2 ppm	5.45 (m, 4H)	8.93 (m, 8H)[a]			4.72 (t, 2H)	
$[Ru(2\text{-}PytB_3P)(PyCN)]_2$ (**5**)	3.11 (d, 2H)	5.76 (d, 4H)	7.76−8.75	1.58 (s)	1.32 (d, 4H)	
	5.16 (t, 2H)	8.36 (d, 4H)		1.65 (s)	3.63 (d, 4H)	
($C_6D_5CD_3$)	5.54 (d, 2H)	8.79 (m, 8H)				
δ/ppm vs $C_6H_5CH_3$ 2.1 ppm	5.62 (t, 2H)					
$[Ru(2\text{-}PyT_3P)(H_23\text{-}PytB_3P)]_2$ (**6**)	3.22 (d, 2H)	5.73 (d, 4H)	6.65−8.63	1.45 (s)	2.30 (d, 2H)	−2.56
	3.64 (t, 2H)	8.25 (d, 4H)		1.47 (s)	4.40 (m, 2H)	
(C_6D_6)	4.40 (m, 2H)	8.78 (d, 4H)		(*tert* - Bu)	6.02 (d, 2H)	
δ/ppm vs C_6H_6 7.2 ppm	4.50 (t, 2H)	8.86 (d, 4H)		2.35 (s)		
		6.74 (d, 4H)		2.45 (s)		
		8.57 (d, 4H)		(tolyl)		
		8.93 (d, 4H)				
		8.99 (d, 4H)				
$[Ru(2\text{-}PyT_3P)(H_24\text{-}PytB_3P)]_2$ (**7**)	3.70 (d, 2H)	6.99 (d, 4H)	8.85−7.04	1.41 (s)	2.29 (d, 4H)	−2.60
	5.23 (t, 2H)	8.43 (d, 4H)		1.45 (s)	5.08 (d, 4H)	
(C_6D_6)	5.67 (t, 2H)	8.85 (m, 8H)		(*tert* - Bu)		
δ/ppm vs C_6H_6 7.2 ppm	5.94 (d, 2H)	6.21 (d, 4H)		2.55 (s)		
		8.54 (d, 4H)		2.58 (s)		
		9.07 (m, 8H)		(tolyl)		

[a] The multiplet signal is due to overlap between the signals of the β-pyrrol and phenyl groups.

observed, clearly excluded the coordination of 4-cyanopyridine by the cyano nitrogen. The ^{1}H NMR data of the perpendicularly linked oligomers[11] and the bispyridine dimer **4** supported the formation of the cofacial dimer **5**, $[Ru(2\text{-}PytB_3P)(NC_5H_4\text{-}CN)]_2$. The infrared spectrum of **5** showed a characteristic sharp stretch band of it's cyano substituents (ν_{CN}) at 2232 cm^{-1}, while ν_{CN} of free 4-cyanopyridine appeared at 2236 cm^{-1}, that is, there was little difference between the two bands. It was noted that when benzonitrile was coordinated to the Ru(II) ion in the pentaammine complexes, the ν_{CN} of free benzonitrile (2231 cm^{-1}) shifted to a significantly lower frequency (2188 cm^{-1}), due to strong π-back-bonding from Ru(II) ion to the cyano substituent.[17] These results also verified that 4-cyanopyridine was coordinated to Ru(II) ion through the nitrogen atom of the pyridyl group instead of the cyano group.

Bispyridylporphyrin Tetramers, 6 and 7. Elemental analyses of **6** and **7** were satisfactory. ESI-MS of **6** and **7** gave fragment peaks of the same molecular weight at m/z^+ 3081.8. Relative abundances of the fragments were 70% for **6** and 100% for **7**. ^{1}H NMR spectra of **6** and **7** revealed that the oligomers took on porphyrin tetrameric structures. In both the tetramers, the ratios of integral intensities between CH_3 (tolyl) and *tert*-butyl proton signals were 1:3, indicating the composition of 1:1 (2:2) for the ruthenium porphyrin and axial porphyrin subunits. Integral intensities of the other proton signals also agreed well with the 1:1 composition. The signals for the pyridyl and β-pyrrole protons of the ruthenium porphyrin and axial porphyrin subunits were observed at high magnetic fields as listed in Table 1. In the case of **7**, four pyridyl proton signals of the cofacial dimer subunits and two pyridyl proton signals of the axial 4-pyridylporphyrin subunits were distinguished by integral intensities and signal correlations obtained by H−H COSY. Although the proton signals of the 2-positions of the axial 3-pyridyl groups of **6** were not assigned by the H−H COSY because of the absence of vicinal couplings, four pyridyl proton signals of the cofacial dimer subunits and three pyridyl proton signals of the axial 3-pyridylporphyrin subunits were assigned. The integral intensities and the other signals assigned to seven pyridyl protons and eight β-pyrrole protons indicated that **6** has the porphyrin tetrameric structure and that the axial porphyrin ligands are rotating around the ruthenium ions in the NMR time scale.

These spectroscopic and analytical results apparently revealed that the ruthenium porphyrin oligomers, **1**−**7**, have cofacial dimeric frameworks and a variety of corresponding axial ligands (CO, Py, PyCN, Py-POR).

Electrochemical Studies. Redox potentials of the cofacial carbonyl ruthenium porphyrin dimers, **1** and **2**, are listed in Table 2. The redox behavior of **1** and **2** were almost the same and very characteristic in the stepwise oxidation of the porphyrin rings owing to the strong interactions between the two porphyrin rings. Both the carbonyl dimers exhibited four one-electron oxidation waves from 650 to 1500 mV (Figure S2). The former two waves and the latter two waves were assigned to the first and second porphyrin ring oxidation processes, respectively. The average redox potentials of the former two waves ($E_{1(av)}$) and those of the latter two waves ($E_{2(av)}$) in both **1** and **2** were not so different from those of the first and second porphyrin oxidation waves of $Ru(tB_4P)(CO)(Py)$. The differences, ($E_{2(av)} - E_{1(av)}$ values), in the average redox potentials of **1** and **2** were 585 and 601 mV, respectively. These values were similar to those of $Ru(tB_4P)(CO)(Py)$ and Ru(TPP)(CO)(Py)[18] as listed in Table 2.

Redox potentials of the cofacial bispyridine porphyrin dimers, **3** and **4**, are listed in Table 3. Figure 2a and b showed that the

(17) (a) Nakamoto, K. *Infrared and Raman Spectra of Inorganic and Coordination Compounds*, 3rd ed.; A Wiley-Interscience: New York, 1978. (b) Clark, R. E.; Ford, P. C. *Inorg. Chem.* **1970**, 9, 227.

Table 2. Redox Potentials $E^{\circ\prime}$ and $\Delta E^{\circ\prime}$ (in mV) Values of Cofacial Carbonyl Dimers[a]

complex	por oxidn. 1 E_1 ($\Delta E^{\circ\prime}$)	por oxidn. 2 E_2 ($\Delta E^{\circ\prime}$)	E_2(av) − E_1(av)
[Ru(2-PyT$_3$P)(CO)]$_2$ (**1**)	660 [1]	1286 [1]	
	(259)	(176)	585
	919 [1]	1462 [1]	
[Ru(2-PytB$_3$P)(CO)]$_2$ (**2**)	662 [1]	1316 [1]	
	(274)	(174)	601
	936 [1]	1482 [1]	
Ru(TPP)(CO)(Py) (vs SSCE)[b]	810	1360	550
Ru(tB$_4$P)(CO)(Py)	675	1246	571

[a] Redox potentials were obtained from $(E_{pa} + E_{pc})/2 (E^{\circ})$. The values were corrected by the potential of a ferrocenium/ferrocene couple (352 mV). The numerals in brackets are the numbers of electrons transferred which were evaluated from the wave heights of CV or DPV. [b] Reference 18a.

redox behavior of **3** and **4** were almost the same, that is, stepwise four one-electron oxidations proceeded in both **3** and **4.** The former two one-electron waves were assigned to Ru(III /II) similar to those of Ru(tB$_4$P)(Py)$_2$ and Ru(TPP)(Py)$_2$.[18] Although the latter two one-electron waves were irreversible processes, the waves could be assigned to the first porphyrin ring oxidation steps.

The potential differences ($\Delta E^{\circ\prime}$, over 270 mV) in each redox process of the cofacial carbonyl and bispyridine dimers were significantly (20 to 60 mV) larger than those of the cyclic tetramers such as [Ru(4-PyT$_3$P)(CO)]$_4$ and [Ru(4-PyT$_3$P)(Py)]$_4$.[19] The strong interactions between the two ruthenium porphyrin subunits in these cofacial dimers apparently result from the proximity between the two ruthenium porphyrin subunits. We believe that the cofacial arrangement and overlapping of the two porphyrin planes, as observed in the X-ray structures of cofacial zinc porphyrin dimers,[6a] are essential for the strong interactions. The redox profile of **5** was similar to those of **3** and **4**, that is, **5** exhibited two reversible one-electron waves of Ru(III/II) and two irreversible one-electron waves of the ruthenium porphyrin ring oxidation processes. The potentials of Ru(III/II) in **5** were shifted to the positive direction relative to that of **4** due to the stronger electron-withdrawing abilities (more strong π-acidity) of the coordinated 4-cyanopyridine. It is interesting that the potentials of the ruthenium porphyrin ring oxidations were negatively shifted, relative to that of **4**. Similar correlation in the potential shifts of Ru(III/II) and the porphyrin ring oxidations was observed between Ru(TBP)(azpy)$_2$ and Ru(TBP)(pyz)$_2$.[20] The redox potential of Ru(III/II) of Ru(TBP)(azpy)$_2$ is more positive than that of Ru(TBP)(pyz)$_2$ and the porphyrin ring oxidation of Ru(TBP)(azpy)$_2$ is more negative than that of Ru(TBP)(pyz)$_2$. These results suggested that the π-acidity of the axial pyridyl ligands controlled the strength of the interaction between the π or π^* orbitals of the porphyrin rings and the d orbitals of the ruthenium ion.

Redox potentials of the tetramers, **6** and **7**, and free axial porphyrin ligands are also tabulated in Table 3. Cyclic voltammograms of **6** and **7** are given in Figure 3a and b. The redox behavior of the axial porphyrin ligands of **6** and **7** was different from that of the free porphyrins H$_2$(3-Py)tB$_3$P and H$_2$(4-Py)tB$_3$P with respect to reversibility. The free ligands show irreversible porphyrin ring oxidation, because the one-electron ring oxidation caused nucleophilic attack of the pyridyl group on the β-positions of the other porphyrin rings to give polymerized species.[21] On the other hand, in the tetramers of **6** and **7**, the polymerization was inhibited by the coordination of the pyridyl groups to ruthenium ions, so that the reversible porphyrin ring oxidation progressed.[11b] Both the complexes, **6** and **7**, exhibited two one-electron waves of the Ru(III/II) processes. Potential differences, $\Delta E^{\circ\prime}$, of the processes were more than 320 mV. These $\Delta E^{\circ\prime}$ values of **6** and **7** were larger than those of **3**−**5** by more than 30 mV. Besides the two Ru(III/II) processes, two additional reversible processes appeared at around 950−1300 mV. Each of these processes apparently mediated 2-electron transfers judging from the current heights in cyclic voltammograms and differential pulse voltammograms as shown in Figures 3 and S3. The processes could be assigned to the overall 2-electron oxidations of each of the axial porphyrin rings, because the cofacial ruthenium porphyrin rings must be oxidized at higher potential regions and the processes must be irreversible as experienced in the systems of **3**−**5**. Namely the results indicated that the two axial porphyrin ligands in each of **6** and **7** were oxidized at the same potentials. Irreversible oxidation waves were actually observed at more positive potentials of 1612 mV for **6** and 1480 mV for **7**. The irreversible waves were assigned to the oxidations of the ruthenium porphyrin rings of **6** and **7**. The shifts to the positive direction in the oxidation processes of the ruthenium porphyrin rings might result from the plus charges on the axial porphyrin ligands. The positive shift of **6** is larger than that of **7**, and could come from the differences in proximity of the ruthenium porphyrins from the π-conjugated systems of the axial porphyrins, that is, **6** is apparently closer than **7**. The difference in the interactions between the core ruthenium porphyrins and the axial porphyrins in these two systems was reflected by the redox potentials in the oxidation steps of the axial porphyrins of **6** (989 mV) and **7** (963 mV), that is, the potentials were the reverse of the free porphyrins H$_2$3-PytB$_3$P (834 mV) and H$_2$4-PytB$_3$P (902 mV).

In the region of negative potentials, redox processes were observed as shown in Figure 3. In the case of **7**, two reduction processes of the axial porphyrin ligands were observed, similar to those of the free 4-pyridylporphyrin, though the redox potentials were shifted slightly in positive direction. The reduction processes of **7** mediated two-electron transfers, indicating that two axial porphyrin ligands are reduced at the same potential with no interactions between the axial porphyrins, which is similar to the case of the perpendicularly arranged porphyrin dimers and trimers.[11b] On the other hand, the redox profile of the reduction processes of the axial porphyrins in **6** was significantly different from that of free 3-pyridylporphyrin as shown in Figure 3a, that is, a reduction wave was observed at −1363 mV in **6**. In addition, the number of electrons transferred in this process was determined to be one by the current ratio between the reduction process and Ru(III/II) processes, suggesting that the two axial porphyrins interact via the cofacial ruthenium porphyrin dimer subunits. This result might be brought about by proximal interactions through the π^* orbitals of the porphyrin π-conjugated systems between the axial 3-pyridylporphyrins and the core ruthenium porphyrins.

(18) (a) Brown, G. M.; Hopf, F. R.; Ferguson, J. A.; Meyer, T. J.; Whitten, D. G. *J. Am. Chem. Soc.* **1973**, *95*, 5939. (b) Felton, R. H. In *The Porphyrins*; Dolphin, D., Ed.; Academic Press: New York, 1979; Vol. 5, Chapter 3. (c) Brown, G. M.; Hopf, F. R.; Meyer, T. J.; Whitten, D. G. *J. Am. Chem. Soc.* **1975**, *97*, 5385. (d) Pacheco, G. M.; James, B. R.; Rettig, S. J. *Inorg. Chem.* **1995**, *34*, 3477.
(19) Funatsu, K.; Imamura, T.; Ichimura, A.; Sasaki, Y. *Inorg. Chem.* **1998**, *37*, 1798.
(20) Marvaud, V.; Launay, J. P. *Inorg. Chem.* **1993**, *32*, 1376.
(21) Giraudeau, A.; Ruhlmann, L.; El Kahef, L.; Gross, M. *J. Am. Chem. Soc.* **1996**, *118*, 2969.

Table 3. Redox Potentials $E^{\circ\prime}$ and $\Delta E^{\circ\prime}$ (in mV) Values of Cofacial Bispyridine Dimers and Tetramers[a]

complex	Ru(III/II) ($\Delta E^{\circ\prime}$)	por oxidn ($\Delta E^{\circ\prime}$)	axial por	
			oxidn.	redn.
$[Ru(2\text{-}PyT_3P)(Py)]_2$ (**3**)	23 [1]	1284 (E_{pa}) [1]		
	(296)	(209)		
	319 [1]	1493 (E_{pa}) [1]		
$[Ru(2\text{-}PytB_3P)(Py)]_2$ (**4**)	15 [1]	1255 (E_{pa}) [1]		
	(290)	(207)		
	305 [1]	1462 (E_{pa}) [1]		
$[Ru(2Py)tB_3P)(PyCN)]_2$ (**5**)	116 [1]	1230 (E_{pa}) [1]		
	(269)	(123)		
	384 [1]	1353 (E_{pa}) [1]		
$[Ru(2\text{-}PyT_3P)(H_23\text{-}PytB_3P)]_2$ (**6**)	10 [1]	1612 (E_{pa})	989 [1 × 2]	−1363 [1]
	(328)		1279 [1 × 2]	
	338 [1]			
$[Ru(2\text{-}PyT_3P)(H_24\text{-}PytB_3P)]_2$ (**7**)	52 [1]	1480 (E_{pa})	963 [1 × 2]	−1580 [1 × 2]
	(321)		1208 [1 × 2]	−1233 [1 × 2]
	373 [1]			
$Ru(TPP)(Py)_2$ (vs SSCE)[b]	210	1260		
$Ru(tB_4P)(Py)_2$	82	1121		
$Ru(tB_4P)(PyCN)_2$	326	1165		
$Ru(OEP)(PyCN)_2$	107	1080		
$H_23\text{-}PytB_3P$			834	−1692
			1138	−1351
$H_24\text{-}PytB_3P$			902	−1648
			1301 (E_{pa})	−1290

[a] Redox potentials were obtained from $(E_{pa} + E_{pc})/2(E^{\circ\prime})$. The values were corrected by the potential of a ferrocenium/ferrocene couple (352 mV). The numerals in brackets are the numbers of electrons transferred, which were evaluated from the wave heights of CV or DPV. [b] Reference 18a.

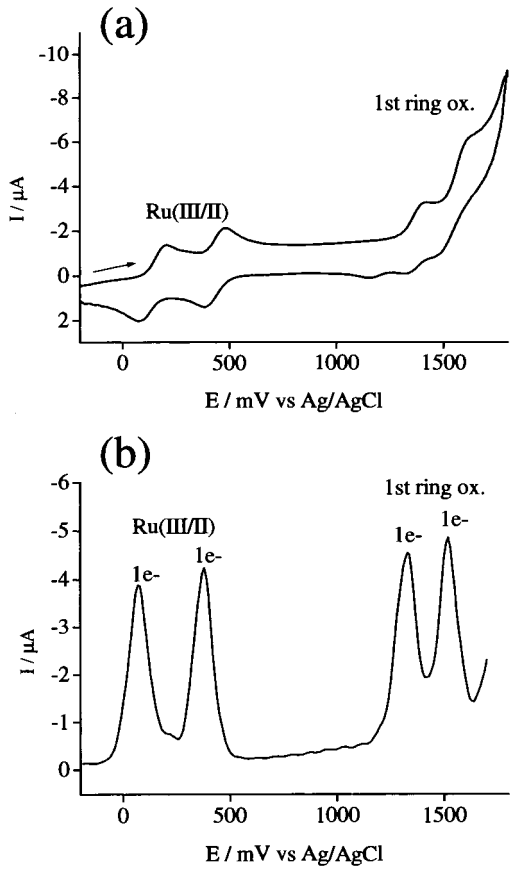

Figure 2. (a) Cyclic voltammogram of $[Ru(2\text{-}PytB_3P)(Py)]_2$ (**4**) in 0.1 M $TBA(PF_6)$ CH_2Cl_2 solution. (b) Differential pulse voltammogram of $[Ru(2\text{-}PytB_3P)(Py)]_2$ (**4**) in 0.1 M $TBA(PF_6)$ CH_2Cl_2 solution.

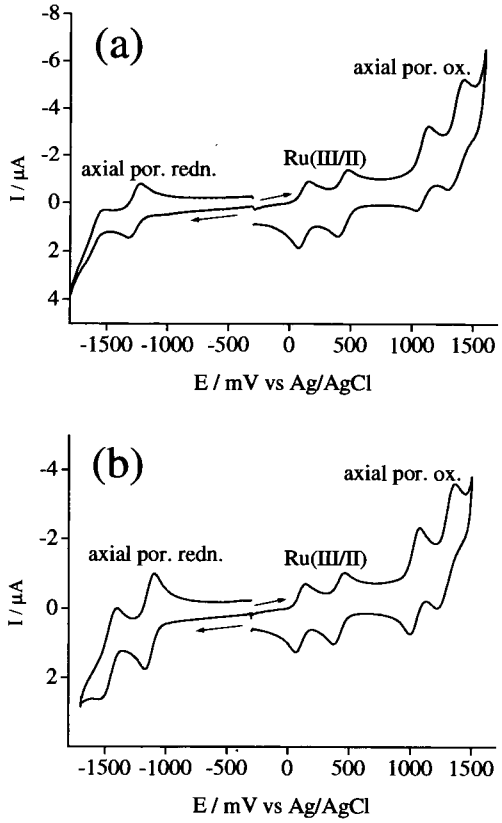

Figure 3. (a) Cyclic voltammogram of $[Ru(2\text{-}PyT_3P)(H_23\text{-}PytB_3P)]_2$ (**6**) in 0.1 M $TBA(PF_6)$ CH_2Cl_2 solution. (b) Cyclic voltammogram of $[Ru(2\text{-}PyT_3P)(H_24\text{-}PytB_3P)]_2$ (**7**) in 0.1 M $TBA(PF_6)$ CH_2Cl_2 solution.

UV−Vis Spectroscopy. UV−vis spectroscopic data are listed in Table 4. UV-vis spectra of the cofacial ruthenium porphyrin dimers were very characteristic. Each of the cofacial carbonyl dimers **1** and **2** exhibited a significant broad Soret band with an absorption maximum at 412 nm as shown in Figure 4. Similar porphyrin dimers $[Zn(2\text{-}PyPOR)]_2$ and an imidazole tethered cofacial zinc porphyrin dimer $[Zn(OEP\text{-}im)]_2$ showed apparent exciton splittings of the Soret bands with a splitting range of 890 to 1040 cm^{-1}.[6a] In contrast, **1** and **2** showed no exciton splittings, though the frameworks of the dimers were

Table 4. UV−Vis Data of Ruthenium Porphyrin Oligomer

complex	solvent	λ_{max}/nm (ϵ; 10^4 M^{-1} cm^{-1}/ϵ per subunit)
[Ru(2-PyT$_3$P)(CO)]$_2$ (**1**)	CH_2Cl_2	413 (22.4/11.2), 539 (3.79/1.90), 579 (0.71/0.36)
[Ru(2-PytB$_3$P)(CO)]$_2$ (**2**)	CH_2Cl_2	413 (23.3/11.7), 539 (4.02/2.01), 575 (0.74/0.37)
[Ru(2-PyT$_3$P)(Py)]$_2$ (**3**)	CH_2Cl_2	403 (19.6/9.8), 421 (sh.), 508 (3.03/1.52)
[Ru(2-PytB$_3$P)(Py)]$_2$ (**4**)	CH_2Cl_2	405 (18.7/9.4), 422 (sh.), 508 (2.83/1.42)
[Ru(2-PytB$_3$P)(PyCN)]$_2$ (**5**)	CH_2Cl_2	403 (17.4/8.7), 418 (17.3/8.7), 508 (3.86/1.93), 621 (1.41/0.71), 665 (1.15/0.58)
[Ru(2-PyT$_3$P)(H$_2$3-PytB$_3$P)]$_2$ (**6**)	$C_6H_5CH_3$	407 (sh. 37.2), 421 (60.9), 516 (6.00), 552 (3.52), 591 (2.03), 650 (1.62)
[Ru(2-PyT$_3$P)(H$_2$4-PytB$_3$P)]$_2$ (**7**)	$C_6H_5CH_3$	407 (sh. 38.9), 421 (73.5), 513 (7.13), 550 (3.41), 589 (2.21), 652 (1.56)
H$_2$3-PytB$_3$P	$C_6H_5CH_3$	420 (46.8), 516 (1.98), 551 (1.03), 593 (0.58), 650 (0.52)
H$_2$4-PytB$_3$P	$C_6H_5CH_3$	420 (45.9), 516 (1.98), 551 (0.95), 591 (0.59), 649 (0.45)
Ru(tB$_4$P)(CO)(Py)	CH_2Cl_2	414 (27.0), 534 (2.05), 568 (0.59)
Ru(tB$_4$P)(Py)$_2$	CH_2Cl_2	413 (16.0), 422 (16.5), 506 (2.29)
Ru(tB$_4$P)(PyCN)$_2$	CH_2Cl_2	407 (sh. 10.1), 418 (20.8), 509 (2.83), 550−650 (broad band)
Ru(OEP)(PyCN)$_2$	CH_2Cl_2	399 (12.1), 498 (1.59), 525 (3.29), 618 (1.69)

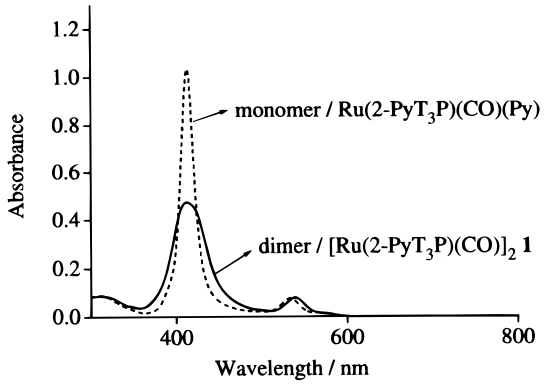

Figure 4. UV-vis spectral change of carbonyl dimer **1** in CH_2Cl_2 by the addition of excess pyridine (100 equiv) at 23 °C.

almost the same as those of the cofacial zinc porphyrin dimers. On addition of a large amount of pyridine to the solutions of **1** and **2**, the Soret bands sharpened and increased in intensity without change in the absorption maxima. The change is due to the pyridine substitution reactions to form the corresponding monomers, Ru(2-PyT$_3$P)(CO)(Py) and Ru(2-PytB$_3$P)(CO)(Py), as shown in Figure 4. The final spectra were almost the same as those of Ru(tB$_4$P)(CO)(Py) and Ru(TPP)(CO)(Py).[15a] Half-widths of the Soret bands of these monomers were ca. 18 nm, which was less than half of the half-widths (45 nm) of **1** and **2**. Furthermore, the absorption intensities of the monomer spectra were more than twice of those of **1** and **2**. These characteristics of the Soret bands in **1** and **2** are likely to result mainly from excitonic interactions between the two porphyrin π-conjugated systems.[22] The Q-bands of **1** and **2** showed red shifts by ca. 250 cm^{-1} relative to those of the corresponding monomers. Similar red shifts (100−150 cm^{-1}) were reported in the systems of the cofacial zinc dimers.

The Soret bands and Q-bands of the bispyridine dimers **3** and **4** were also significantly broad relative to those of the corresponding monomers, Ru(2-PyT$_3$P)(Py)$_2$ and Ru(2-PytB$_3$P)-(Py)$_2$. In addition, the Soret bands of **3** and **4** were blue shifted by 7−9 nm relative to the corresponding monomers. Figure 5 shows the characteristic UV−vis spectrum of bis(4-cyanopyridine) dimer **5**. The Soret band and Q-band were also significantly broadened relative to the corresponding monomer of Ru(tB$_4$P)(PyCN)$_2$. Although the feature of the porphyrin $\pi - \pi^*$ transition (the Soret band and Q-band) of **5** was similar to those of **3** and **4**, extra broad bands were observed for **5** at 621 and 665 nm. These bands were also observed for monomer analogues of Ru(tB$_4$P)(PyCN)$_2$ (550−650 nm) and Ru(OEP)-(PyCN)$_2$ (618 nm) as shown in Figure 5a and Table 4. From the facts described later, the bands were assigned to a metal to ligand charge-transfer band (MLCT: Ru(dπ) − cyanopyridine-(π^*)). The bands exhibited solvent dependence, e.g., the band of **5** shifted from 614 nm in toluene (dielectric constant: 2.4) to 621 nm in dichloromethane (8.9) and 625 nm in acetone (20.7).[23] The oxidation of Ru(II) to Ru(III) in these three biscyanopyridine complexes using $(NH_4)_2Ce(NO_3)_6$ as an oxidizing agent decreased the intensities of the bands as shown in Figure 5b. Ru(OEP)(Py)$_2$ exhibits a MLCT band (Ru(dπ) − Py(π^*)) at around 450 nm, because the eight ethyl substituents of the OEP rings with electron donating abilities raise the e_g^* orbitals of the porphyrins above the lowest pyridine π^* orbital.[24] On the other hand, the MLCT bands were not observed for Ru-

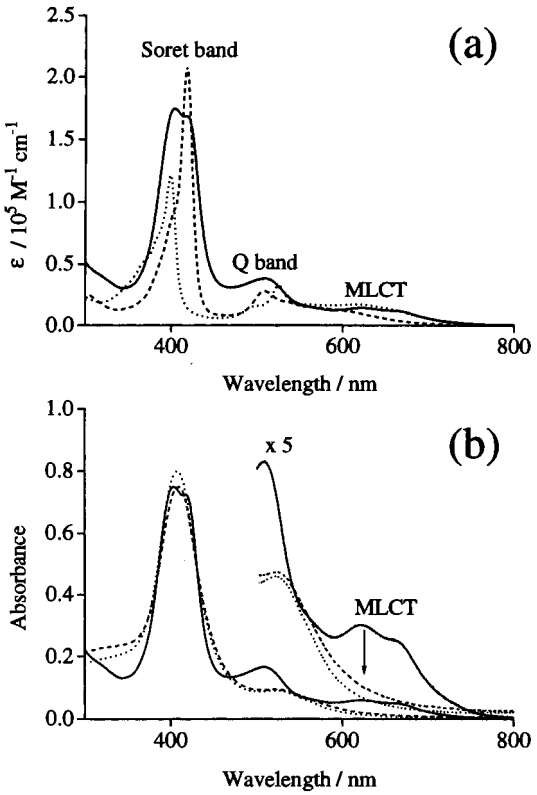

Figure 5. (a) UV−vis spectra of bis(4-cyano)pyridine dimer and monomers in CH_2Cl_2 at 23 °C. Solid line: [Ru(2-PytB$_3$P)(PyCN)]$_2$ (**5**). Dashed line: Ru(tB$_4$P)(PyCN)$_2$. Dotted line: Ru(OEP)(PyCN)$_2$. (b) UV−vis spectral changes of [Ru(2-PytB$_3$P)(PyCN)]$_2$ **5** by one electron oxidative titration with Ce(IV) in CH_2Cl_2 at 23 °C. Solid line: [Ru^{II,II}-(2-PytB$_3$P)(PyCN)]$_2$. Dashed line: [Ru^{II,III}(2-PytB$_3$P)(PyCN)]$_2^+$. Dotted line: [Ru^{III,III}(2-PytB$_3$P)(PyCN)]$_2^{2+}$.

(22) (a) Kasha, M.; Rawls, H. L.; El-Bayoumi, M. A. *Pure Appl. Chem.* **1965**, *11*, 371. (b) Kasha, M.; *Radiat. Res.* **1963**, *20*, 55.

(23) Wollmann, H. *Pharmazie* **1974**, *29*, 708.

(TPP)$(Py)_2$ because the four *meso*-phenyl substituents are electron-withdrawing and stabilize the e_g* orbitals of the porphyrin below the pyridine π* orbital.[24] The lowest π* orbital of 4-cyanopyridine with an electron-withdrawing cyano group must be lower than the lowest π* orbital of pyridine. Thus the shift of the MLCT band (Ru(dπ) − cyanopyridine(π*)) of Ru(OEP)$(PyCN)_2$ (618 nm) to lower energy relative to the Ru(OEP)$(Py)_2$ systems (450 nm) is rationalized. In addition, since the lowest π* orbital of 4-cyanopyridine may be below the e_g* orbitals of the *meso*-arylporphyrin rings of tB_4P and 2-PytB_3P, MLCT bands (Ru(dπ) − cyanopyridine(π*)) were observed for **5** (621 nm) and Ru(tB_4P)$(PyCN)_2$ (550−650 nm). In fact, a ruthenium(II) *meso*-tetraarylporphyrin complex having two axial azopyridine ligands, Ru(TBP)$(azpy)_2$, exhibited the MLCT band (Ru(dπ) − azpy(π*)) in the lower energy region at around 800 nm, since the lowest π* orbital of azopyridine is more stable than those of 4-cyanopyridine and pyridine.[20]

UV−vis spectra of the porphyrin tetramers **6** and **7** were measured in toluene, because these tetramers were unstable in dichloromethane. In both the tetramers, four peaks of the Q-bands of the axial porphyrin ligands were observed in the region of 500−650 nm as shown in Table 4 and Figure S4. Q-bands due to the core cofacial ruthenium porphyrin subunits should also be in this region, though no peaks were observed. Besides the Q-bands, another broad band was observed for **7** at around 650−750 nm. Similar broad bands appeared in the same region in previously reported perpendicularly linked porphyrin trimers, Ru(OEP)($H_2$4-PyP_3P)$_2$ and Ru(TTP)($H_2$4-PyP_3P)$_2$.[11b]

In both **6** and **7,** the Soret bands of the ruthenium porphyrin dimer core and the axial porphyrin subunits overlapped with each other. Although the Soret bands of the ruthenium porphyrin dimer core and the axial porphyrin ligands appeared at 407 nm as a shoulder and 421 nm, respectively, the molar absorptivities of **6** and **7** at 421 nm (60.9×10^4 for **6** and 73.5×10^4 M^{-1} cm^{-1} for **7**) were much smaller than the values expected for two axial porphyrin subunits (larger than 90×10^4 M^{-1} cm^{-1}), even despite overlapping of the Soret bands of the ruthenium porphyrin dimer subunits to some extent. Similar decreases in molar absorptivity have also been commonly observed in perpendicularly linked porphyrin trimers, Ru(OEP)($H_2$4-PyP_3P)$_2$ and Ru(TTP)($H_2$4-PyP_3P)$_2$.[11b] In addition, the decrease in the absorptivity of **6** was much larger than that of **7**. It may be more feasible for π-conjugated systems of the axial 3-pyridylporphyrin ligands to interact with those of the ruthenium porphyrin dimer subunits than between perpendicularly coordinated 4-pyridylporphyrins and the ruthenium porphyrin dimer subunits.

Properties of Mixed-Valence State. As described in the section "Electrochemical Studies", the cofacial dimers and tetramers exhibited stepwise oxidations at the ruthenium porphyrin rings or metal centers due to strong interactions between the cofacially arranged ruthenium porphyrin subunits. The comproportionation constants (Kc) of the mixed-valence dimers estimated from ΔE values (mV) were 2.4×10^4 and 3.3×10^4 for **1** and **2** in the first porphyrin ring oxidation processes, respectively. The constants were also evaluated to be 3.5×10^4, 8.0×10^4, 10.0×10^4, 35.1×10^4, and 26.7×10^4, in the Ru(III/II) processes for **3**, **4**, **5**, **6**, and **7**, respectively. These values indicated that their mixed-valence states (one-electron oxidized complexes) were stable with respect to disproportionation.[25]

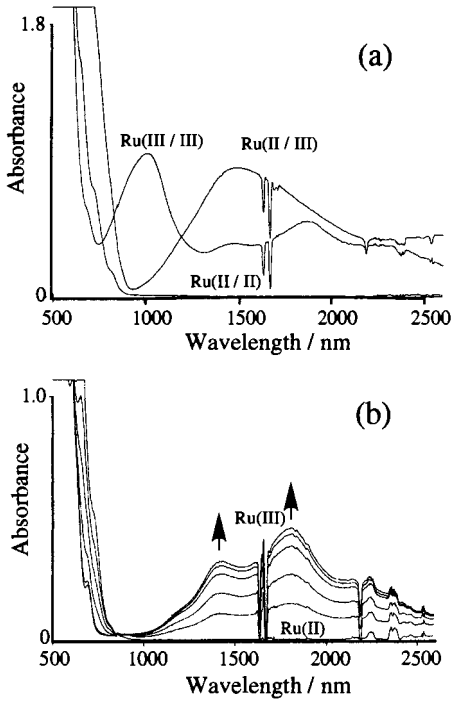

Figure 6. (a) Near−infrared absorption spectral changes in the systems of [Ru(2-PytB_3P)(Py)]$_2$ (**4**) accompanied by one-electron oxidative titration with Ce(IV) in CH_2Cl_2 at 23 °C. (b) Near−infrared absorption spectral change of Ru(TPP)$(Py)_2$ by stepwise 0.25-electron oxidative titrations with Ce(IV) in CH_2Cl_2 at 23 °C. Two spiky peaks at around 1650 nm were doubly generate vibrations of the stretches of C−H bonds in CH_2Cl_2.

Since bulk electrolysis in some cofacial dimers caused adsorption on the electrodes, these dimers were chemically oxidized by Ce(IV) or I_2 to yield the corresponding dimers with mixed valence states. In the cases of the cofacial carbonyl dimers of **1** and **2**, low solubility of the neutral dimer complexes and instability of the mixed-valence states interfered with the measurements of clear visible and near-IR spectra for the mixed-valence states. In **3**, **4**, and **5**, visible and near-IR spectral changes accompanied by oxidative titrations with Ce(IV) or I_2 were followed successfully. The spectral changes in **3** and **4** matched to the theoretical stoichiometries. On the other hand, in **5**, the oxidizing agents needed more than a stoichiometric amount to obtain the mixed valence state species, because of the high redox potentials of Ru(III/II) in these systems. The visible spectral change in the system of **4** caused by the oxidations of ruthenium ions was similar to that of **5** except that the spectral change occurred at around 600 nm. The visible spectra of the one- and two-electron oxidized complexes derived from **4** or **5** almost returned to the initial spectra of the parent complexes on reduction by cobaltcene.

Spectral change of **4** and Ru(TPP)$(Py)_2$ in the near-IR regions by the titrimetric oxidation with Ce(IV) are shown in Figure 6a and b, respectively. Although both the dimer and the neutral monomer had no bands in the region of 1000−2500 nm, one-electron oxidation of **4** gave a new broad band in the near-IR region with a peak maximum at 1500 nm. The broad band increased in intensity on addition of Ce(IV) and attained maximum intensity with the stoichiometric addition for complete

(24) (a) Schick, G. A.; Bocian, D. F. *J. Am. Chem. Soc.* **1984**, *106*, 1682. (b) Vitols, S. E.; Roman, J. S.; Ryan, D. E.; Blackwood, M. E., Jr.; Spiro, T. G. *Inorg. Chem.* **1997**, *36*, 764.

(25) Richrdson, D. E.; Taube, H. *Inorg. Chem.* **1981**, *20*, 1278.

one-electron oxidation. Then the broad band decreased upon further addition and finally disappeared to give new two bands between 1500 and 2500 nm. The end point of the completion of the spectral changes fitted the stoichiometry for the two-electron transfer. The spectrum of the two-electron oxidized complex of **4** with two weaker peaks at 1500−2500 nm was similar to that of $[Ru^{III}(TPP)(Py)_2]^+$. These results revealed that the characteristic broad band at 1500 nm of the one-electron oxidized complex was an intervalence charge-transfer (IT) band. Similar broad bands were also observed for the other cofacial dimers, whose peak maxima were 1491 nm for **3** and 1570 nm for **5**. Porphyrin tetramers of **6** and **7** gave also broad bands at around 1500 nm in the course of oxidation. However addition of oxidizing agents to solutions containing **6** or **7** caused simultaneous oxidation of the axial porphyrin ligands besides the oxidation of the ruthenium ions. In fact, the solution of fully oxidized **6** or **7** gave a new visible spectrum with a Soret band at around 445 nm, indicating the formation of π cation radicals derived from the axial porphyrin ligands.[26]

Many mixed valence multinuclear metal complexes such as Creutz−Taube ions show IT bands in the near-IR region.[27] Interactions between the metal centers occur across the conjugated bridging ligands. The dπ(metal) − pπ*(bridging ligand) interactions are important factors to strengthen the interactions between metal centers.[27,28] There are dπ(Ru) − pπ*(porphyrin) interactions in the Ru(POR)$(Py)_2$ systems.[24] Furthermore, in the systems of **3**−**7**, electronic communication of the π-conjugate system between the ruthenium porphyrin rings and 2-pyridyl substituents must be cut off, because of the perpendicular geometries between the porphyrin planes and the 2-pyridyl rings. Hence intervalence charge transfer (IT) between Ru(II) and Ru(III) in **3**−**7** most likely occurs across the overlapping pyrrole rings of the two ruthenium porphyrin rings through the π* orbitals of the ruthenium porphyrin rings.

Figure 6a also shows that the two-electron oxidized complexes in the systems of **3**−**7** have prominent bands at around 1000 nm which were not observed in $[Ru^{III}(TPP)(Py)_2]^+$. Although the origin of the bands is not clear, we tentatively assigned the bands to LMCT from the porphyrin rings arranged cofacially to Ru(III).

Conclusion

A variety of cofacial ruthenium porphyrin dimers, **1**−**5**, with axial CO, pyridine, or 4-cyanopyridine ligands, and tetramers, **6** and **7**, with axial pyridylporphyrin ligands were synthesized. These new oligomers were characterized mainly by spectral methods such as ^{1}H NMR and ESI-MS measurements. Electrochemical properties of the oligomers were characteristic. Oxidations of the porphyrin rings or the ruthenium ions at the first stages proceeded stepwise by the strong interactions between the cofacial dimer subunits. Splittings in the redox potentials (ΔE, mV) were over 260 mV for all oligomers. An interaction between the axial 3-pyridylporphyrin ligands in **6** was observed in the reduction process of the axial 3-pyridylporphyrins, which was in contrast to the noninteracting axial 4-pyridylporphyrin ligands in **7**. Important factors of the strong interaction of the oligomers are the cofacial arrangement between constituent porphyrin planes and the overlap of the π-conjugated systems of the porphyrin rings. Interactions between the porphyrin subunits were represented in UV−vis spectra by significant broadenings in the Soret bands, though apparent exciton splittings were not observed in contrast to the zinc dimers, $[Zn(2\text{-PyPOR})]_2$ and $[Zn(\text{im-POR})]_2$. In **5** and the monomer analogues, Ru(OEP)$(PyCN)_2$ and Ru(tB_4P)$(PyCN)_2$, MLCT bands from Ru(II) to the axial cyanopyridine ligands were observed. Mixed-valence states (Ru(III,II)) in the systems of **3**−**7** exhibited intervalence charge-transfer bands in the near-IR region at around 1500 nm. The intervalence charge transfer most likely proceeds across the overlapping pyrrole rings of the two ruthenium porphyrin rings.

Acknowledgment. We acknowledge funds from a Grant-in-Aid for Scientific Research from the Ministry of Education, Science, Sports and Culture, Japan (No. 08454206) and the 1994 Kawasaki Steel 21st Century Foundation.

Supporting Information Available: Figures of H−H COSY of **4**, cyclic voltammogram of **1**, differential pulse voltammogram of **6**, and UV−vis spectra of **6** and **7** (Figures S1, S2, S3, and S4) (4 pages). Ordering information is given on any current masthead page.

IC971361R

(26) (a) Peychal-Heiling, G.; Wilson, G. S. *Anal. Chem.* **1971**, *43*, 545. (b) Peychal-Heiling, G.; Wilson, G. S. *Anal. Chem.* **1971**, *43*, 550.
(27) (a) Creutz, C.; Taube, H. *J. Am. Chem. Soc.* **1973**, *95*, 1086. (b) Creutz, C. *Prog. Inorg. Chem.* **1983**, *30*, 1. (c) Ward, M. D. *Chem. Soc. Rev.* **1995**, 121.
(28) (a) Ernst, S.; Kasack, V.; Kaim, W. *Inorg. Chem.* **1988**, *27*, 1146. (b) Kaim, W.; Kasack, V. *Inorg. Chem.* **1990**, *29*, 4696.